PERMAFROST - Seventh International Conference (Proceedings),
Yellowknife (Canada), Collection Nordicana No 55, 1998

A NUMERICAL MODEL FOR THE ORGANIZATION OF ICE-WEDGE NETWORKS

L.J. Plug[1,2], B.T. Werner[1]

1. Complex Systems Laboratory
Institute of Geophysics and Planetary Physics
University of California, San Diego
La Jolla, California 92093-0225

2. Alaska Quaternary Center
University of Alaska, Fairbanks
Fairbanks, Alaska 99775
e-mail: plug@shackleton.ucsd.edu

Abstract

Ice-wedge networks organize through feedbacks between thermal tensile stresses in permafrost and the developing fracture pattern. Questions concerning fracture geometry and pattern evolution require a modeling approach that includes time development of networks, the influence on fracture of complicated patterns of stress owing to pre-existing fractures, and the effects of stochastic material properties. To model an ice-wedge network through time, we simulate the development of the fracture pattern on a lattice in plan view. Modeled tensile stress in a cell is a function of pre-fracture thermal stress and position and orientation of nearby fractures. Fractures are initiated in randomly chosen cells exceeding a threshold of tensile stress, and propagation proceeds until a cell is reached where modeled stress falls below strength. The distributions of fracture spacing and relative orientation in model-generated networks closely resemble distributions from mature ice-wedge networks at two sites in northwest Alaska.

Introduction

Ice-wedge networks (Figure 1) are widespread in periglacial landscapes; networks currently span tens of thousands of square kilometers of sub-Arctic and Arctic regions and the surface expression of now-melted wedges from the last glacial period is evident in the Northern Hemisphere as far south as central England and the Midwestern United States (Black, 1969; Johnson, 1990). Currently identified taxonomic categories of ice-wedge networks include random orthogonal, oriented orthogonal, and nonorthogonal (crude hexagons) (Lachenbruch, 1966). Spacing between parallel ice wedges typically ranges from 10 to 50 m and has been hypothesized to vary predictably with substrate properties and winter temperatures (Dostavolov and Popov, 1966).

Whereas considerable evidence has accumulated that thermal contraction cracking (Leffingwell, 1915) is the mechanism for the genesis and growth of a single ice wedge (e.g., Black, 1954; Mackay, 1974), the development and testing of models for the processes underlying network organization are incomplete. The formation of closed polygons has been attributed to the general nature of contraction cracking (Leffingwell, 1915), a hypothesis in which polygonal figures arise through simultaneous opening of bounding fractures. A

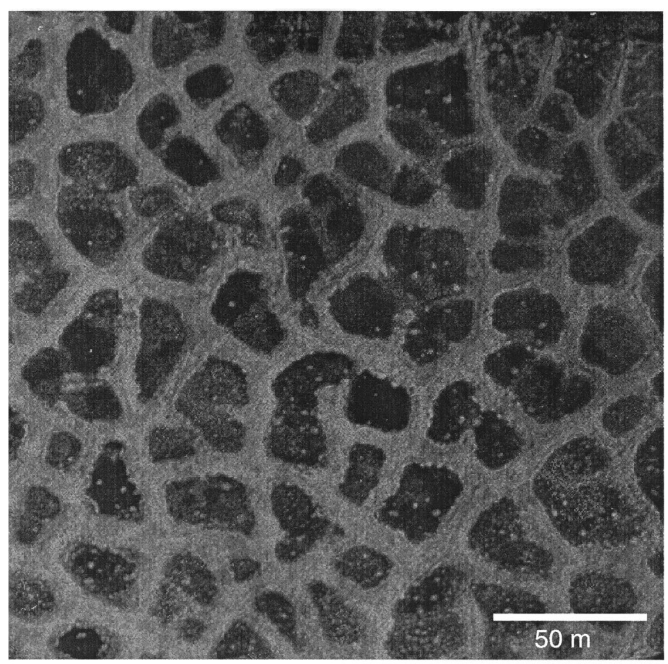

Figure 1. Aerial photograph of a low-centred, random orthogonal ice-wedge network developed in loess near the mouth of the Espenberg River, Alaska.

more specific hypothesis for network organization is the influence of an existing fracture on the tensile stress experienced by a new, propagating fracture (Lachenbruch, 1962; 1966). Hypotheses regarding network development are difficult to test because of the thousands-of-years time scale over which networks evolve.

The initiation and propagation of fractures depend nonlinearly on the placement of neighbouring fractures, variables coupled to the developing ice-wedge pattern (e.g., snow accumulation around wedges), and variables not interacting with the ice-wedge pattern (e.g., snow cover, severity of cooling episodes and material and thermal properties) (Mackay, 1993b). Therefore, approaches based on the Griffith energy-balance theory of fracture (Lachenbruch, 1962) generally do not lead to robust predictions of timing and location of fracture in networks (Mackay, 1993a; 1993b). To model the evolution of ice-wedge networks, the context of the network for each individual fracture and the influence of spatial and temporal variability must be included.

A rule-based model can be used to address complicated, non-uniform behaviour by simplifying small scale dynamics (e.g., Landry and Werner, 1994). Here, we describe a rule-based model for the development of ice-wedge networks and present preliminary results. In the model, (1) the fracturing medium, frozen ground, is projected onto a two-dimensional, plan-view grid; (2) the effects of existing cracks on the tensile stress field, and therefore on subsequent fracture, are encapsulated into simple dynamical rules; and (3) material heterogeneity is parameterized.

Model description

Modeled ice-wedge networks evolve on a two-dimensional lattice composed of square cells with periodic (toroidal) boundary conditions (Figure 2). Cells either are unoccupied or contain a fracture characterized by an angle specifying the direction in which the fracture propagated through the cell. Initially, all cells are unoccupied. Each cell is assigned a value for tensile strength, which is the minimum stress for fracture initiation.

The two-dimensional lattice combines representation of the top of the permafrost, where existing ice wedges often initiate re-fracturing, and the ground surface, where new fractures originate (Mackay, 1983; 1986). Underlying this representation is the assumption that contraction fractures penetrate to approximately uniform depth. This assumption is supported by observations that fractures in wedges generally are three to five meters deep (Mackay, 1974) and wedges in non-aggrading sediment are similar in depth. One explanation for this observed consistency in fracture depth is that fracture propagation might be limited by the presence of a less brittle stratum at depth, owing to an increase in temperature with depth in the ground and dissimilarity between temperature (and hence stress) variations at the surface and at depth. The sensitivity to the assumption of uniform fracture depth is illustrated by the calculated result that tensile stress at the surface rises to within five percent of its pre-fracture value 11.6 m from a 3 m-deep fracture, 19 m from a 6 m-deep fracture, and 22 m from a 9.2 m-deep fracture, assuming the same pre-fracture distribution of stress (Lachenbruch, 1962).

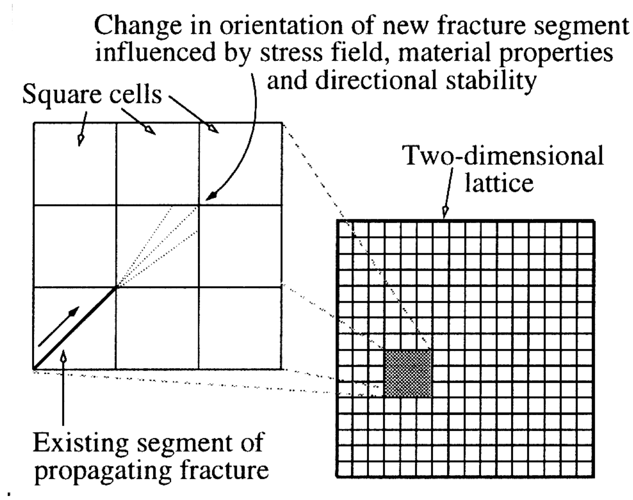

Figure 2. Modeled fractures initiate and propagate on a two-dimensional lattice of 400 by 400 square cells with periodic boundary conditions.

The development of networks is modeled iteratively, where an iteration is the initiation and propagation of a new fracture on the lattice. A fracture remains on the lattice during all subsequent iterations. This approach, which assumes that new fractures in permafrost occur after existing ice wedges have re-fractured, is supported by measurements indicating ice is generally weaker than frozen sediments (Frost Effects Laboratory, 1952). The effect of snow accumulation in reducing the likelihood that an ice wedge overlain by a large trough re-fractures (Mackay, 1974) is not currently modeled.

Fracture Algorithm

Initiation

In the model, an iteration begins by selecting the location of the cell and initial propagation direction of a potential new fracture according to one of two strategies (1) random choice; or (2) a choice that maximizes the ratio of tensile stress to strength. A fracture is initiated if stress normal to the propagation direction exceeds the local tensile strength; otherwise, a new iteration begins.

Propagation

A fracture propagates from the originating cell into neighbouring cells along two opposing directions. The

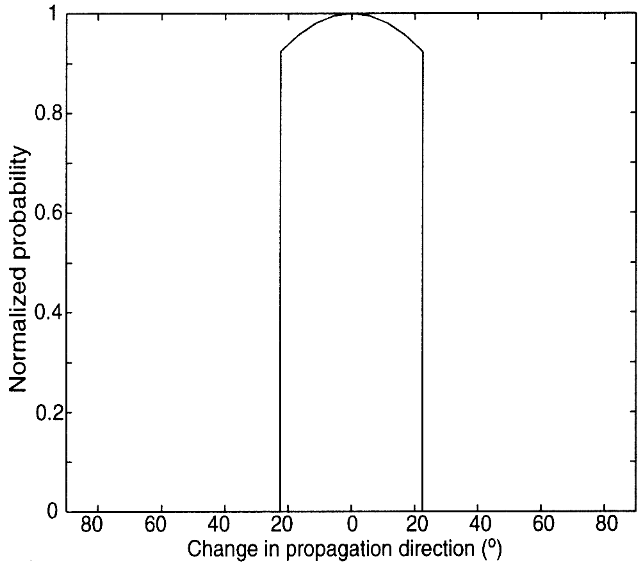

Figure 3. The probability distribution parameterizing the directional stability of a propagating fracture normalized by the probability that the propagation angle does not change.

direction of propagation is re-evaluated as the fracture enters a new cell, according to the inherent directional stability of a fracture, local variations in tensile stress and small-scale (less than cell size) material heterogeneity. A propagating fracture tends to continue in a straight line because this maximizes the release rate of potential strain energy into mechanical energy (Lawn, 1993). This tendency is modeled here by treating a calculated mechanical-energy-release-rate function as the probability that a fracture will change direction in a cell (restricted to the range of +/- 22°) (Figure 3). We are continuing to evaluate the suitability of this approach and the sensitivity of results to different probability distributions. The preferred propagation orientation is the angle *a* that maximizes *D(a)S(a)*, where *D(a)* is the distribution shown in Figure 3 and *S(a)* is the modeled stress (see next section). The effect of variations in strength on scales smaller than cell size is modeled by choosing the change in direction (with respect to the preferred orientation) from a normal distribution, with the standard deviation of the distribution parameterizing the level of material heterogeneity. A fracture propagates until modeled tensile stress falls below tensile strength or the length of the fracture exceeds the edge length of the simulation. This maximum fracture length is imposed to prevent early-generation fractures from propagating beyond one edge of the lattice and reappearing on another edge (owing to periodic boundaries) repeatedly. Beyond the first few model iterations, the length of fractures in modeled networks is not sensitive to this value.

MODELED STRESS

The primary component of stress influencing fracture, normal to the propagation direction, is assessed as a fracture enters an unoccupied cell. The effects of fractures in individual cells j on τ_i, the stress in cell i, are summed linearly, giving

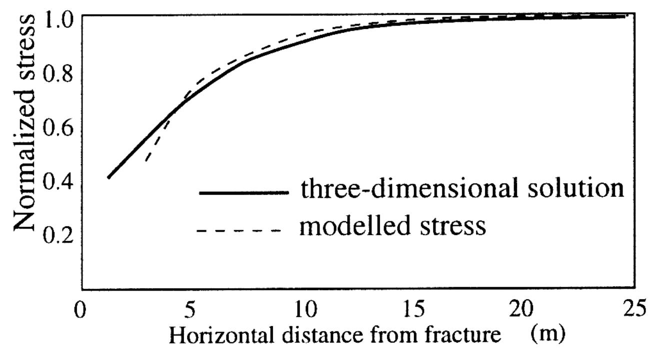

Figure 4. Tensile stress, perpendicular to fracture and normalized by pre-fracture stress, versus the distance from a fracture. The modeled tensile stress (dotted line) is close to a three- dimensional solution for a 6 m deep fracture (Lachenbruch, 1961) for distances greater than 5 m.

$$\tau_i = \tau_{T_i}\left(1 - \sum_{j=1}^{n} R_{ij}\right) \quad [1]$$

where R_{ij} is the fraction of pre-fracture tensile stress in cell i relieved by the presence of a fracture in cell j and τ_{Ti} is the thermal tensile stress in cell i prior to fracture. The functional dependence of an existing fracture segment in cell j on the tensile stress experienced by a fracture segment in cell i is approximated as

$$R_{ij} = \frac{k}{d_{ij}^{n}}\cos\left(\theta_{ij}\right) \quad [2]$$

where d_{ij} is the distance between cells i and j, θ_{ij} is the relative orientation between the two fracture segments, n is an adjustable exponent and k is a scaling factor that varies with the cell size used in the simulation. The solution to the analytical three-dimensional equations for stress perpendicular to a 6m deep fracture is well-approximated with n = 2 and k = 5 (Figure 4). The sensitivity of fracture spacing and intersection orthogonality to variations in the form of equation (2) is a topic of ongoing investigation.

The modeled networks discussed here evolve on a 400 by 400 lattice of one by one meter cells. Thermal stress before fracture is homogenous and normalized to one. The fracture strength for initiation and propagation is $0.4\tau_{Ti}$, where $\tau_{Ti}\tau_{Ti}$ is the pre-fracture stress. The location and orientation of fracture initiation are chosen randomly. The effects of smaller-than-cell-size heterogeneity on propagation direction are parameterized with a normal probability distribution with a standard deviation of 5.6°, a value which is consistent with our field observations of isolated fractures near the Espenberg site and observations of initial contraction

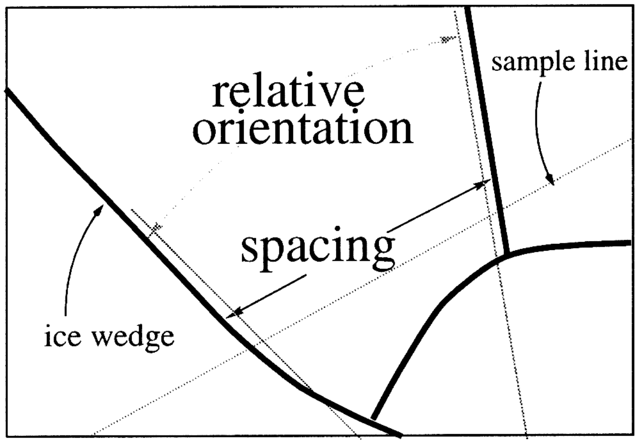

Figure 5. Method used to acquire distributions of fracture spacing and relative orientation.

fractures in frozen ground in the Northwest Territories (Mackay, 1986).

Ice-wedge networks in Alaska

Ice-wedge networks at two locations in northern Alaska are used for comparison to model results: near Cape Espenberg on the Seward Peninsula in Bering Land Bridge National Preserve and near the Mesa Archaeological Site in the northern foothills of the Brooks Range. Both sites are on old surfaces that were not ice-covered during the Wisconsin glaciation. Ice-wedge networks at the sites are well developed; therefore, they are suitable for comparison to mature model networks. The Espenberg site is an upland surface with a random orthogonal network that has developed in ice-rich Pleistocene loess (Hopkins, 1983). Polygons at the site are high-centered; the surfaces between wedges are domed upward and covered with dry tussock tundra vegetation, whereas troughs with more mesic vegetation overlie the ice wedges. Exposures along a retreating river bluff on a high terrace of the Itivluk River near the Mesa Archaeological Site reveal ice wedges three to five meters deep that have developed in an ice-rich sandy-silt substrate. Polygons at the site are high-centered and vegetation is similar to the Espenberg locale.

At the Mesa Archaeological Site, images of ice-wedge networks were acquired from a helicopter hovering at an elevation of 300 m using a remote controlled camera mounted to a skid. Near-infrared, 1:6000-scale aerial photographs from the National Park Service were used for the Espenberg study area. The networks were digitized by relying on the surface expression of ice wedges (primarily moisture and vegetation differences) to delineate the network pattern. Ice wedges that have not caused visible surface deformation or localized changes in soil moisture, because of infrequent fracture or small widths, might be missed using this procedure. Because wedges only influence the thermal stress field following fracture, the influence of infrequently fracturing wedges on network development probably is minor.

Analysis of networks

The spacing and relative orientation of fractures were measured at intersections between fractures and sample line segments. Sample lines dissect the network at randomly selected angles and originate from randomly selected locations on the periphery of the network (Figure 5). Spacing is the distance between two successive intersections with fractures, measured along the sample line. Relative orientation is the absolute value of the angle between successive fractures.

Results

Modeled networks (example in Figure 6) approach a steady-state after 5000 iterations (the increase in the number of cells occupied by fractures from 5000 to 7500 iterations is less than 0.5%) and are visually similar to networks at the Espenberg and Mesa sites (Figure 7).

Fracture Length

The length of new fractures decreases as the modeled network evolves (Figure 8). Early-generation fractures propagate through a largely isotropic tensile stress field because existing fractures are widely spaced and thermal stress remains near its pre-fracture value. Within approximately 300 iterations, the length of individual

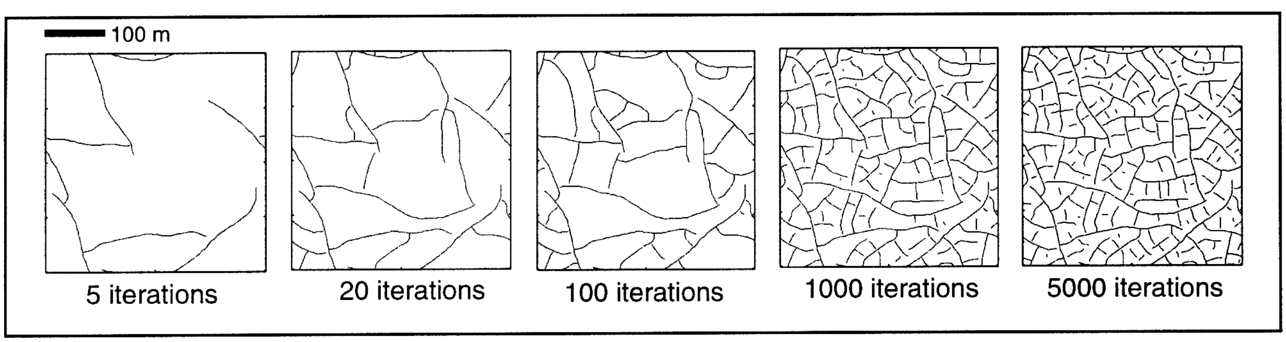

Figure 6. Development of a modeled fracture network over 5000 iterations. Fractures formed early are long and sinuous with gentle bends. Fractures first enclose regions of the simulation space after 20 to 100 iterations, but the dimensions of these regions are several times the width of the spacing of parallel fractures at 5000 iterations. After 1000 iterations, regions enclosed by early-generation fractures have been subdivided by short, often straight fractures for which orientation is determined by early-generation fractures.

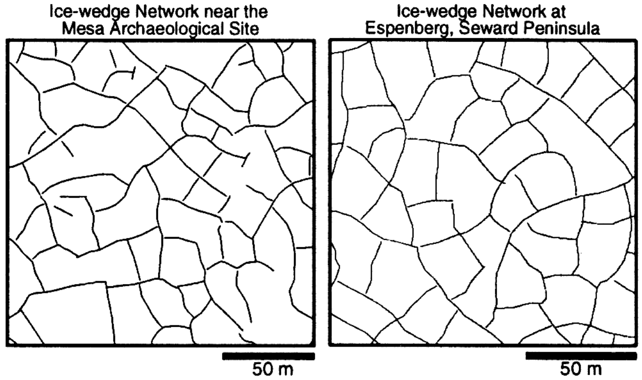

Figure 7. Maps of ice-wedge networks near the Mesa Archaeological Site and Cape Espenberg.

fractures decreases rapidly as the network is increasingly dissected and interactions between fractures, via the consequent pattern of stress, become significant. These results are consistent with field observations that early fractures are long (Mackay, 1986).

Fracture Sinuosity

The degree of and mechanism underlying fracture sinuosity varies as the modeled network evolves. Early fractures are characterized by small and irregular changes in orientation resulting from small-scale heterogeneity in material strength. Some later fractures form small-radius-of- curvature bends in response to anistropic stress fields in the neighbourhood of preexisting cracks. Most late-generation fractures are short, straight segments oriented perpendicular to longer, early-generation fractures.

Comparison between Field Networks and Steady-State Model Networks

Frequency distributions of the relative orientation and spacing of fractures from a steady-state modeled network are qualitatively similar to networks near the Mesa Archaeological Site and Cape Espenberg (Figure 9). Field and modeled networks display orthogonality;

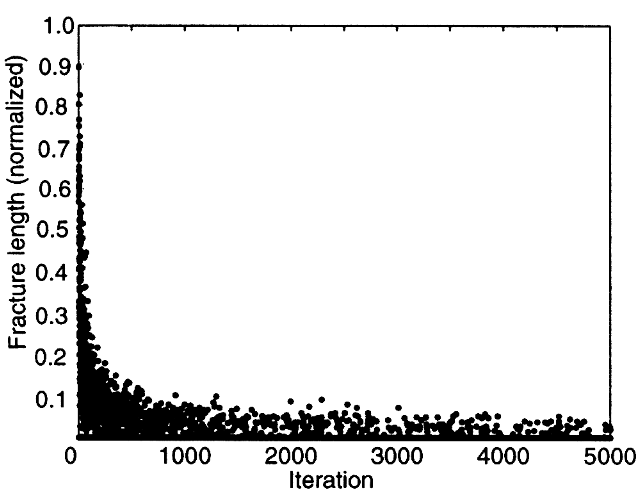

Figure 8. Fracture length (normalized against the edge length of the lattice:400 m) vs. model iteration. Fracture length decreases with iteration.

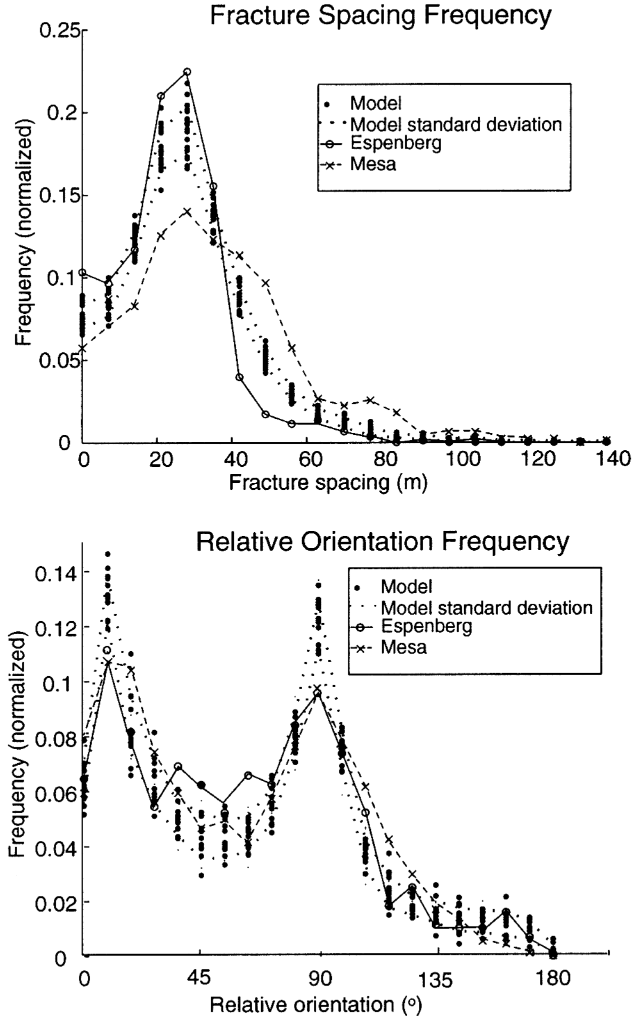

Figure 9. Distribution of fracture spacing and relative orientation for ice-wedge networks in Alaska (near Cape Espenberg, Seward Peninsula, and near the Mesa Archaeological Site, North Slope) and twenty modeled networks after 5000 iterations.

relative orientations of fractures are bimodally distributed with peaks at 5% and 90%. Model predictions of 25 to 30 m for fracture spacing are consistent with the spacing of ice wedges in the Espenberg and Mesa networks and greater than a prediction of 20 m between two parallel fractures 6 m deep (Lachenbruch, 1962). The two measured field networks are not statistically consistent with a sample population of twenty modeled networks. However, the differences between the Espenberg and Mesa ice-wedge networks are similar to the mean of the differences between both field networks and each of twenty realizations of the model. Specifically, the standard deviation of the residuals for the fracture spacing distributions are as follows: Espenberg-Mesa, 0.044 m^{-1}; Espenberg-model, 0.021 m^{-1}; Mesa-model, 0.027 m^{-1}, with 7 m bins. For relative orientation, the standard deviation of the residuals are: Espenberg-Mesa, 0.012 deg^{-1}; Espenberg-model, 0.016 deg-1; Mesa-model, 0.016 deg^{-1}, with 9° bins.

Discussion

A rule-based model employing simplifications of the stress-field in the neighbourhood of fractures and of crack-tip dynamics produces fracture networks geometrically similar to two ice-wedge networks in Alaska. The initial results suggest that many of the features of ice-wedge networks might be insensitive to the detailed dynamics of fracture. Future work will include investigating the sensitivity of network properties to model assumptions, more detailed comparisons between modeled and ice-wedge networks, and investigation of network evolution under varying climates and substrate properties.

Acknowledgments

This study was supported by the National Science Foundation, Arctic Natural Sciences Program (OPP-9530860) and the National Park Service, Bering Land Bridge National Preserve, Beringian Shared Heritage Program. The Bureau of Land Management, Alaska region, provided logistical support at the Mesa Archaeological Site. Dan Mann provided helpful advice and assistance in the field. David Hopkins introduced L. Plug to the geomorphology of the Cape Espenberg region.

References

Black, R.F. (1954). Permafrost -- a review. *Geological Society of America Bulletin*, **65**, 839- 855.

Black, R.F. (1969). Climatically significant fossil periglacial phenomena in north central United States. *Biuletyn Peryglacjalny*, **20**, 225-238.

Dostovalov, B.N. and Popov, A.A. (1966). Polygonal systems of ice wedges and conditions of their development. In *Proceedings 1st International Conference on Permafrost*. National Research Council of Canada, Ottawa, Publication 1287, pp. 102-105.

Frost Effects Laboratory, U.S. Army Corps of Engineers (1952). *Investigation, description, classification and strength properties of frozen soils*. SIPRE Report 8 (88 pp).

Hopkins, D.M. (1983). Aspects of paleogeography of Beringia during the late Pleistocene. In Hopkins D.M., Matthews, J.V., Schweger, C.E., and Young, S.B. (eds.), *Paleoecology of Beringia*. Academic Press, New York, pp. 3-28.

Johnson, W.H. (1990). Ice-wedge casts and relict patterned ground in central Illinois and their environmental significance. *Quaternary Research*, **33**, 51-72.

Lachenbruch, A.H. (1961). Depth and Spacing of Tension Cracks. *Journal of Geophysical Research*, **66**, 4273-4292.

Lachenbruch, A.H. (1962). Mechanics of thermal contraction cracks and ice-wedge polygons in permafrost. *Geological Survey of America Special Paper*, **70** (69 pp).

Lachenbruch, A.H. (1966). Contraction theory of ice-wedge polygons: a qualitative approach. In *Proceedings 2nd Permafrost International Conference*, NAS-NRC Publication 1287 63-71.

Lawn, B.R. (1993). *Fracture of Brittle Solids*. Cambridge University Press, Cambridge (378 pp).

Landry, W. and Werner, B.T. (1994). Computer simulations of self-organized wind ripple patterns. *Physica D*, **77**, 238-260.

Leffingwell, E. de K. (1915). Ground-ice wedges, the dominant form of ground-ice on the north coast of Alaska. *Journal of Geology*, **23**, 635-654.

Mackay, J.R. (1974). Ice-wedge cracks, Garry Island, Northwest Territories. *Canadian Journal of Earth Sciences*, **11**, 1366-1383.

Mackay, J.R. (1983). The direction of ice-wedge cracking in permafrost: downward or upward? *Canadian Journal of Earth Sciences*, **25**, 516-524.

Mackay, J.R. (1986) The first 7 years (1978-1985) of ice wedge growth, Illisarvik experimental drained lake site, western Arctic coast. *Canadian Journal of Earth Sciences*, **23**, 1782-1795.

Mackay, J.R. (1993a). The sound and speed of ice-wedge cracking, Arctic Canada. *Canadian Journal of Earth Sciences*, **30**, 509-518.

Mackay, J.R. (1993b). Air temperature, snow cover, creep of frozen ground, and the time of ice-wedge cracking, western Arctic coast. *Canadian Journal of Earth Sciences*, **30**, 1720-1729.